

## Phase Separation in a Chaotic Flow

Ludovic Berthier,<sup>1,2</sup> Jean-Louis Barrat,<sup>1</sup> and Jorge Kurchan<sup>3</sup>

<sup>1</sup>*Département de Physique des Matériaux, Université C. Bernard and CNRS, F-69622 Villeurbanne, France*

<sup>2</sup>*Laboratoire de Physique, ENS-Lyon and CNRS, F-69007 Lyon, France*

<sup>3</sup>*PMMH, École Supérieure de Physique et Chimie Industrielles, F-75005 Paris, France*

(Received 17 October 2000)

The phase separation between two immiscible liquids advected by a bidimensional velocity field is investigated numerically by solving the corresponding Cahn-Hilliard equation. We study how the spinodal decomposition process depends on the presence—or absence—of Lagrangian chaos. A fully chaotic flow, in particular, limits the growth of domains, and for unequal volume fractions of the liquids, a characteristic exponential distribution of droplet sizes is obtained. The limiting domain size results from a balance between chaotic mixing and spinodal decomposition, measured in terms of Lyapunov exponent and diffusivity constant, respectively.

DOI: 10.1103/PhysRevLett.86.2014

PACS numbers: 47.52.+j, 05.70.Ln, 47.55.Kf, 64.75.+g

A system of two immiscible fluids at rest will gradually phase separate, forming domains whose size grows algebraically with time. Everyday experience, however, shows that by continuously stirring or shaking the fluids the domains or droplets of the phases (say, oil and vinegar) break and coalesce, leading to a dynamic stationary state with domains of finite size.

A first approach consists of modeling this situation by subjecting the binary fluid to a homogeneous shear velocity field [1]. However, experiments [2], numerical simulations [3], and more recently analytical approaches [4] show that in such a situation infinitely long domains aligned with the flow are formed. The effect of the velocity field is to counter the Rayleigh instability, stabilizing *lamellar* and (in certain cases) even cylindrical domains [5,6]. Domain breakup in those situations takes place only at large Reynolds numbers, and is generally attributed to inertial effects [1,7]. Studying these inertial effects numerically is difficult, as a realistic description of the feedback of domain shape on the flow is required [7]. The corresponding simulations are therefore limited by finite size effects.

In this Letter, we investigate a different mechanism by which domains of finite size can be stabilized in a demixing system. In particular, we show that a saturation of the average length scale takes place even in the absence of inertial effects if the flow has *Lagrangian chaos* (i.e., if the trajectories of nearby starting points diverge exponentially

with time). This is interesting for two reasons: First, with an appropriate time dependence of the velocity field one can still have Lagrangian chaos in a situation of high viscosity in which inertial effects are negligible—this is how one mixes pastes. Second, it is possible in that case to decouple the hydrodynamic problem from the phase separation. This problem of a *passive, phase separating scalar field* is, of course, much simpler, so that simulations using large systems are possible. Our approach therefore extends earlier extensive studies of *passive scalar* advection by periodically driven chaotic flows [8].

Our study is also related in spirit to earlier studies of advection by “synthetic” velocity fields tuned to model turbulent flows [9,10]. Phase separation was studied in this context in Ref. [11]. An essential difference, compared to our work, is that in such turbulent flows the separation between nearby tracer particles appears to increase algebraically, rather than exponentially, with time.

We consider a two dimensional flow that can be tuned to be regular, mixed, or fully chaotic. Specifically, the incompressible velocity field  $\mathbf{v}(x, y, t)$  is a modified version of the so-called time-dependent Harper map [12] (related to the “partitioned-pipe mixer,” a special case of “eggbeater flow” [8]). The dynamics takes place on a square of side  $L$ , with periodic boundary conditions. The velocity field is an alternating sequence of shears in the  $x$  and in the  $y$  direction with a time period  $T$ ,

$$\begin{aligned} v_x &= -\frac{2\pi\alpha L}{T} \sin\left(\frac{2\pi y}{L}\right); & v_y &= 0; & n < \frac{t}{T} < n + \frac{1}{2}, \\ v_y &= \frac{2\pi\alpha L}{T} \sin\left(\frac{2\pi x}{L}\right); & v_x &= 0; & n + \frac{1}{2} < \frac{t}{T} < n + 1. \end{aligned} \quad (1)$$

The parameter  $\alpha$  controls the chaoticity of the trajectories. If  $\alpha$  is small, the two semicycles are composed into the smooth, laminar velocity field:  $v_x = -\frac{\pi\alpha L}{T} \sin(\frac{2\pi y}{L})$ ;  $v_y = \frac{\pi\alpha L}{T} \sin(\frac{2\pi x}{L})$ . For larger values of  $\alpha$  the trajectories stretch and fold, and the flow becomes chaotic. In

order to visualize this, it is convenient to follow the position of a point at the end of each cycle. This “kicked Harper” map is shown in Fig. 1 for several values of  $\alpha$ . For  $\alpha \sim 0.2$  the flow is a mixture of laminar and chaotic regions, and becomes fully chaotic around  $\alpha \sim 0.4$ . In

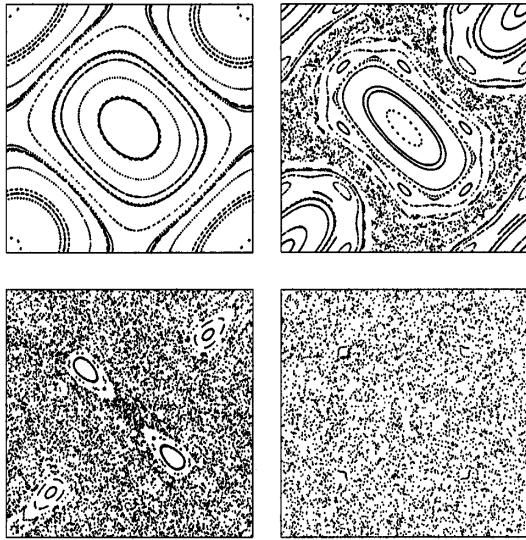


FIG. 1. The maps obtained from snapshots at intervals  $T$  of the lines of current with the dynamics (1), starting from various initial conditions. Figures for  $\alpha = 0.1$  (top left), 0.25, 0.4, and 1.0 (bottom right).

the chaotic situation, it is convenient to characterize the flow by the Lyapunov exponent  $\lambda$ , defined by the fact that nearby starting points separate as  $\sim e^{\lambda t}$ . We have computed  $\lambda$  as in Ref. [10] and found that the relation  $\lambda \approx 1.96 \ln(3.35\alpha)/T$  is a good approximation throughout the chaotic regime,  $\alpha \gtrsim 0.4$ .

The spinodal decomposition of the two-component fluid is described by the Cahn-Hilliard equation

$$\frac{\partial \phi(\mathbf{r}, t)}{\partial t} + \mathbf{v}(\mathbf{r}, t) \cdot \nabla \phi(\mathbf{r}, t) = \Gamma \nabla^2 \left( \frac{\delta F[\phi]}{\delta \phi(\mathbf{r}, t)} \right). \quad (2)$$

Here  $\phi$  is a dimensionless concentration field, the concentrations of the species are  $[1 \pm \phi]/2$ . We work at  $T = 0$ , since temperature is irrelevant in this process [13]. The free energy functional is of the Ginzburg-Landau form and reads

$$F[\phi] = \int d^d \mathbf{x} \left[ \frac{\xi^2}{2} (\nabla \phi)^2 - \frac{1}{2} \phi^2 + \frac{1}{4} \phi^4 \right]. \quad (3)$$

Here  $\xi$  is the equilibrium correlation length controlling the width of the interfaces, and  $d$  is the number of spatial dimensions. We consider the following two topologically different situations: (i)  $\langle \phi \rangle \neq 0$ : a species is less abundant than the other and forms disconnected droplets, and (ii)  $\langle \phi \rangle = 0$ : the two phases are in equal quantity and form a bicontinuous structure. Situation (i) has been studied experimentally [14].

In a chaotic flow, the passive scalar mixes rapidly, whereas in the case of phase separation this tendency is opposed by surface tension. The competition between these two effects can be quantified through two adimensional parameters,  $D \equiv \Gamma T / \xi^2$  (the adimensional

transport coefficient of the Cahn-Hilliard equation) and the chaoticity parameter  $\alpha$ , or alternatively the adimensional Lyapunov exponent  $\lambda T$ . A large  $D$  means that appreciable diffusive transport will take place during each laminar half cycle. A large  $\lambda T$ , on the other hand, means that the mixing process is efficient within a few cycles. Note that  $\lambda$  can also be interpreted as an average elongation or shear rate experienced by the fluid particles.

Equation (2) is integrated numerically with the velocity field (1), using the implicit spectral method developed and discussed in Ref. [15]. The results are presented with time and length units chosen as the cycle period  $T$  and the interfacial thickness  $\xi$ , respectively. The system size, lattice parameter, and time step are  $L = 512\xi$ ,  $\Delta x = \xi$ , and  $\Delta t = 5 \times 10^{-4} T$ , respectively.

*Existence of a stationary state.*—We first show that a purely chaotic flow does, indeed, stop the domain growth. In Fig. 2, we show the evolution of a phase-separated sample with  $\langle \phi \rangle = 1/2$ , upon turning on a chaotic velocity field ( $\alpha = 0.4$ ). The large droplets of the initial configuration are broken into smaller droplets, until a stationary state where droplets successively grow and break is reached. Figure 3 shows the late stages of coarsening of a system with equal concentrations of phases ( $\langle \phi \rangle = 0$ ) in the four velocity fields of Fig. 1. For  $\alpha = 0.1$ , the velocity field is laminar. We observe in that case structures very similar to those found in a homogeneous shear flow, but which now follow the winding flow lines. In the mixed case,  $\alpha = 0.25$ , large-domain structures form in the laminar regions of the flow, and break into very small domains in the chaotic ones. In the fully chaotic situation,  $\alpha \gtrsim 0.4$ , a dynamical stationary state is reached, with small domains continuously breaking and reforming. For  $\alpha = 1.0$ , the sinusoidal nature of the underlying velocity field

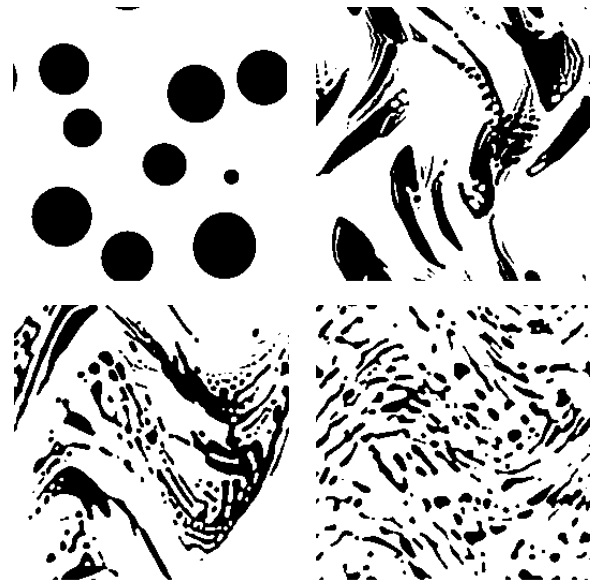


FIG. 2. Evolution of an assembly of large droplets in the chaotic flow for times  $t = 0, 0.65, 1.50$ , and 11.8.

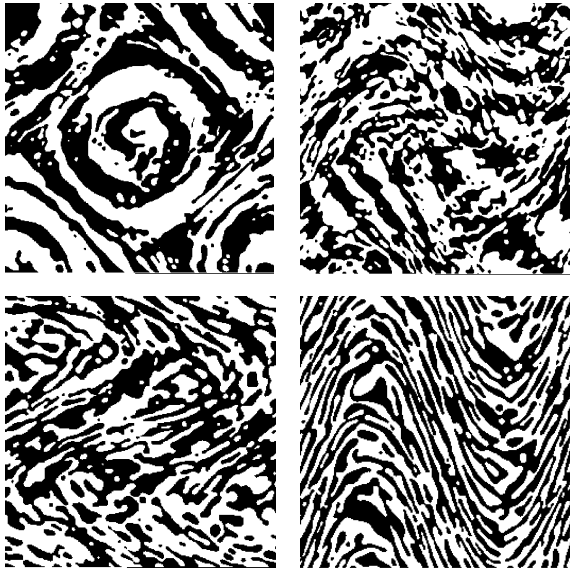


FIG. 3. Late stages of coarsening in the velocity fields of Fig. 1, in the same order.

becomes apparent. This snapshot nicely illustrates the typical “stretch and fold” processes characteristic of chaotic advection [8].

*Scaling properties in the chaotic flow.*—In the stationary regime, it is clear from Figs. 2 and 3 that there exists a typical length scale  $L^*$  which depends on the parameters  $D$  and  $\lambda$ : this will be confirmed below by a quantitative analysis. As in the pure coarsening case [13], scaling properties are expected in the regime  $\xi \ll L^*(D, \lambda) \ll L$ . The length scale  $L^*$  may be estimated by the following simple argument. In the absence of flow, the domains grow as  $L(t)/\xi \approx (Dt/T)^{1/3}$ , and this growth is stopped by the chaotic flow which introduces a time scale  $\lambda^{-1}$ . Hence, we estimate  $L^* \approx L(t = \lambda^{-1})$  and predict

$$L^*(D, \lambda) \approx \xi \left( \frac{D}{\lambda T} \right)^{1/3}. \quad (4)$$

*Isolated droplets,  $\langle \phi \rangle \neq 0$ .*—Following Ref. [14], we characterize the assembly of droplets by computing the distribution of droplet surfaces  $f(S)$ , where  $f(S) dS$  is the probability that the surface occupied by a droplet is between  $S$  and  $S + dS$ . In the scaling regime, we expect this distribution to be of the form

$$f(S) \approx \frac{1}{S^*} \mathcal{F}\left(\frac{S}{S^*}\right), \quad (5)$$

where  $S^*$  is a typical droplet area. In Fig. 4, data obtained for a wide range for the values of  $D$  and  $\lambda$  are collapsed by using a reduced variable  $S/S^*$ , with  $S^* \approx (D/\lambda)^{0.62}$ . The data collapse is satisfactory, and the result for  $S^*$  reasonably close to what would be expected from Eq. (4), i.e.,  $S^* \approx (D/\lambda)^{2/3}$ . Finding an exponent slightly smaller than the one expected theoretically is not surprising, since the typical domain sizes are rather small ( $S^* \lesssim 50\xi^2$ ), so that the asymptotic value for the domain growth exponent

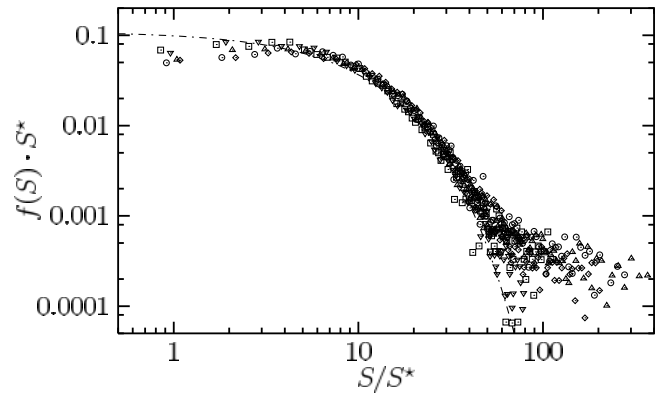


FIG. 4. Surface distribution of the droplets rescaled according to Eq. (5), where the typical surface  $S^*$  is given by  $S^* \approx (D/\lambda)^{0.62}$ . The dot-dashed line is a fit to an exponential form, and the data are for a range  $\alpha \in [0.4, 3.0]$  and  $D \in [100, 2000]$ .

in the absence of flow may not be reached. The rescaled distribution functions exhibit an exponential tail,  $\mathcal{F}(y) \sim e^{-y}$  (dot-dashed line in Fig. 4). Such distributions are very similar to those found in the experiments of Ref. [14]. For the largest droplets, deviations from the exponential fit are observed, indicating either insufficient statistics or a different scaling behavior for the extreme values of  $S$ .

*Equal concentrations:  $\langle \phi \rangle = 0$ .*—In the case of equal concentrations, the domains are ramified and extend throughout the sample, so that the area is not a useful measure of domain size. A characteristic domain size can nevertheless be obtained from the two-point correlation function  $C(\mathbf{r}, t) \equiv L^{-2} \int d^2\mathbf{x} \langle \phi(\mathbf{x}, t) \phi(\mathbf{x} + \mathbf{r}, t) \rangle$ , which is the Fourier transform of the structure factor measured in light scattering experiments. Performing a time average over many configurations shows that the bicontinuous structure is on average perfectly isotropic, as it is in the absence of flow. One can therefore average  $C(\mathbf{r}, t)$  over orientations to obtain a one variable function,  $C(r)$ . The characteristic domain size  $L^*$  can be defined by  $C(L^*) = 0.5$ . Figure 5 displays this domain size for various combinations of  $D$  and  $\lambda$ , as a function of the ratio  $D/\lambda$ . The data can be fitted by  $L^* \approx \xi(D/\lambda T)^{0.27}$ .

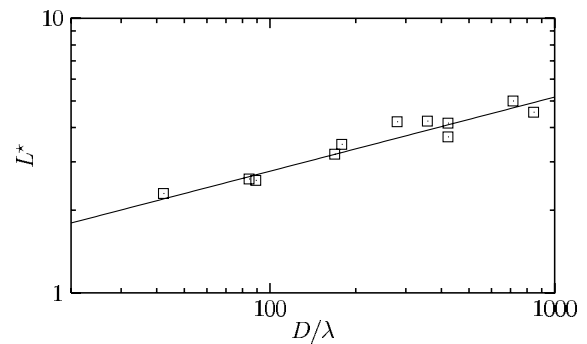


FIG. 5. Log-log plot of the typical domain size  $L^*$  as a function of the ratio  $D/\lambda$  for the same values for  $D$  and  $\alpha$  as in Fig. 4. The full line has a slope 0.27.

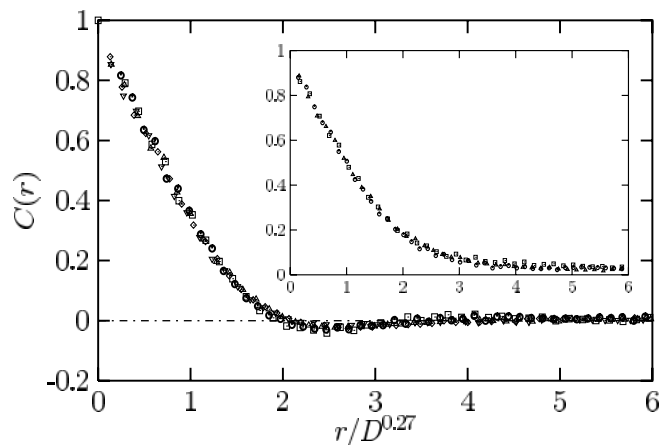


FIG. 6. Two-point correlation function  $C(r)$  at fixed  $\alpha$  for various mobility  $D$ , as a function of the rescaled variable  $r/D^{0.27}$ . Main:  $\alpha = 1.0$  and  $D = 100, 200, 400, 1000$ , and  $2000$ . Inset:  $\alpha = 0.4$  and  $D = 100, 200$ , and  $400$ .

Again, this is in reasonable agreement with the scaling analysis, Eq. (4). Larger simulations, with smaller values of  $\lambda$ , would be necessary to obtain larger domain sizes and avoid the crossover effects which are well known in spinodal decomposition simulations [13].

More detailed information on the domain structure is obtained from the full correlation function  $C(r)$ . Here one could expect from the scaling hypothesis a behavior of the form

$$C(r) \approx C\left(\frac{r}{L^*}\right) \quad (6)$$

with  $C$  a universal function. This hypothesis is tested in Fig. 6, where  $C(r)$  is represented for fixed  $\lambda$  and various values of  $D$ . At fixed  $\lambda$ , a good collapse of the data obtained for different  $D$  is achieved by using a rescaled variable  $r/D^{0.27}$ . The inset of Fig. 6, however, shows that the shape of the scaling function slightly depends on  $\lambda$ , so that the universal scaling expressed by Eq. (6) is not valid. We attribute this change of the scaling function with the flow pattern to the fact that even in the chaotic regime the flow cannot be considered as being homogeneous and isotropic, but exhibits an underlying sinusoidal structure. This is in contrast with the case of isolated droplets where the droplet distribution was not affected by this structure; recall Fig. 4.

We have studied the phase separation in conditions in which the species boundaries are passively advected by an incompressible flow. We have shown that a chaotic flow results in a steady state with domains of finite size resulting from the balance between spinodal decomposition and

chaotic advection, Eq. (4). This should be contrasted with the situation observed in turbulent flow, where the flow intensity must exceed a threshold in order to stop domain growth [11]. Such a difference can be traced back to the fact that Lyapunov exponents for passive scalar advection are actually 0 in the latter case. The essential approximation in our work, compared to realistic experimental situations, is the assumption that the flow pattern is not modified by the domain growth. This assumption, however, may not be unrealistic if the two fluids have similar viscosities and if the capillary stresses are small compared to viscous stresses. This is measured by the capillary number  $C_a = \eta\lambda/(\gamma/L^*)$ , where  $\eta$  is the viscosity and  $\gamma$  the surface tension. In highly viscous fluids,  $C_a$  is expected to be large, so that the decoupling is possible. This decoupling also makes it possible to consider analytical treatments.

We acknowledge useful discussions with A. J. Bray, B. Cabane, P. Leboeuf, J. F. Pinton, and J. E. Wesfreid.

- 
- [1] A. Onuki, *J. Phys. Condens. Matter* **9**, 6119 (1997).
  - [2] T. Hashimoto, K. Matsuzaka, E. Moses, and A. Onuki, *Phys. Rev. Lett.* **74**, 126 (1995).
  - [3] F. Corberi, G. Gonnella, and A. Lamura, *Phys. Rev. Lett.* **81**, 3852 (1998); L. Berthier, e-print cond-mat/0011314.
  - [4] A. Cavagna, A. J. Bray, and R. D. M. Travasso, *Phys. Rev. E* **62**, 4702 (2000).
  - [5] A. Frischknecht, *Phys. Rev. E* **56**, 6970 (1997); **58**, 3495 (1998).
  - [6] Droplet formation in three dimensions at high dilution may happen at times long enough to destabilize cylindrical domains, but too short to form lamellar domains.
  - [7] A. J. Wagner and J. M. Yeomans, *Phys. Rev. E* **59**, 4366 (1999); M. E. Cates, V. M. Kendon, P. Bladon, and J.-C. Desplat, *Faraday Discuss.* **112**, 1 (1999).
  - [8] J. M. Ottino, *Annu. Rev. Fluid. Mech.* **22**, 207 (1990); J. M. Ottino *et al.*, *Nature (London)* **333**, 419 (1988); H. Aref, *J. Fluid. Mech.* **143**, 1 (1984); J. M. Ottino *et al.*, *Science* **257**, 754 (1992).
  - [9] M. Holzer and E. Siggia, *Phys. Fluids* **6**, 1820 (1994).
  - [10] A. Babiano, G. Boffetta, A. Provenzale, and A. Vulpiani, *Phys. Fluids* **6**, 2465 (1994).
  - [11] A. M. Lacasta, J. M. Sancho, and F. Sagués, *Phys. Rev. Lett.* **75**, 1791 (1995).
  - [12] V. N. Govorukhin, A. Morgulis, V. I. Yudovich, and G. M. Zaslavsky, *Phys. Rev. E* **60**, 2788 (1999), and references therein.
  - [13] A. J. Bray, *Adv. Phys.* **43**, 357 (1994).
  - [14] F. J. Muzzio, M. Tjahjadi, and J. M. Ottino, *Phys. Rev. Lett.* **67**, 54 (1991).
  - [15] L. Berthier, J.-L. Barrat, and J. Kurchan, *Eur. Phys. J. B* **11**, 635 (1999).